

GeV Scale Inelastic Dark Matter with Dark Photon Mediator via Direct Detection and Cosmological/Laboratory Constraints

HONG-JIAN HE,^{1,2,3,*} YU-CHEN WANG,^{2,†} and JIAMING ZHENG^{1,‡}

¹*Tsung-Dao Lee Institute & School of Physics and Astronomy,
Shanghai Key Laboratory for Particle Physics and Cosmology,
Shanghai Jiao Tong University, Shanghai 200240, China*

²*Institute of Modern Physics & Physics Department, Tsinghua University, Beijing 100084, China*

³*Center for High Energy Physics, Peking University, Beijing 100871, China*

We propose a new candidate of GeV scale inelastic dark matter (DM). Both the DM particles and the first family fermions are charged under a dark $U(1)_X$ gauge group. Our construction is highly testable and receives nontrivial experimental constraints, including the limits by the DM relic abundance, the lifetime of the heavier DM component, the collider searches, and the electroweak precision data. Under these constraints, we resolve the recent XENON1T anomaly via electron recoil detection, and predict the inelastic DM mass to be $\lesssim 1$ GeV. We further study the light DM constraints from the nuclear recoil detection by the CRESST-III experiment.

I. Introduction

Searching for GeV scale light dark matter (DM) particles is a challenging task, and measuring the DM-electron recoil energy can provide an important means for the light DM direct detection. The XENON collaboration [1] recently announced a 3.5σ excess of events with low electron recoil energy in its Science Run-I [2]. The XENON1T detector recorded 285 events for the recoil energy $E_R = (1-7)$ keV, among which the expected background events are 232 ± 15 [2]. The excess mostly centers around $E_R = (2-3.5)$ keV. In addition, the PandaX-II collaboration also reported an independent DM search by measuring the low energy electron recoil spectrum with robust estimates of background [3]. But, the sensitivity is not yet enough to either confirm or rule out the DM explanations of the XENON1T anomaly. There have been possible explanations for the XENON1T excess in the literature, including unexpected Tritium background [2, 4] and various new physics models [5-8].

One attractive resolution of the XENON1T anomaly is the exothermic inelastic scattering [7, 8] between the DM and electron. In this scenario, the DM consists of two components (X, X') with a small mass-splitting $\Delta m \equiv m_{X'} - m_X$, which is around the anomalous recoil energy region (2-3) keV of XENON1T. The heavier DM component X' is cosmologically stable because its decay to the lighter DM component X can be highly suppressed by the small mass-splitting Δm . Inside the xenon detector, X' scatters inelastically with the xenon electron and deexcite to X . The DM mass-splitting manifests itself as a peak in the electron recoil energy spectrum. On the other hand, the recoil energy from the elastic DM-electron scattering is too small to be detectable in XENON1T unless the DM particles are very fast moving [5]. To generate the

XENON1T anomaly, we can estimate the required normalized cross section of the DM-electron inelastic scattering, $\bar{\sigma}_e/m_{X'} \approx 8.8 \times 10^{-44} \text{cm}^2/\text{GeV}$, assuming that the DM consists of equal amount of (X, X'). Here we define $\bar{\sigma}_e \equiv \sigma_{Xe}(|\mathbf{q}| = 0)$, which denotes the scattering cross section of $X'e^- \rightarrow Xe^-$ in the zero-momentum-exchange limit $|\mathbf{q}| = 0$.

In the literature, the exothermic inelastic scattering was mostly realized by exchanging a very light dark photon which couples to leptons by assuming a tiny kinetic mixing between the dark photon and the standard model (SM) photon [7]. These models require a large hierarchy between the dark photon-lepton couplings and the dark photon-DM coupling. As such, the dark photons could be hidden from various collider searches by tuning its small lepton couplings. But it is actually not necessary to assume such tiny kinetic mixing between the vector mediator and the photon to realize the desired DM-electron recoil signals and satisfy the cosmological/laboratory bounds at the same time.

In this work, we propose a renormalizable inelastic DM model in which both the DM and the right-handed fermions in the first family are charged under a dark $U(1)_X$ gauge symmetry. Because the dark photon mediator couples directly to electrons, we drive non-trivial constraints by various laboratory measurements, such as the anomalous electron dipole moment and mono-photon searches in e^+e^- colliders. We show that this model is viable for the DM and mediator having masses smaller than a few GeV. It can provide the observed DM relic abundance and ensure the heavier DM component to be cosmologically stable. It can generate the observed XENON1T electron recoil spectrum. We can achieve the desired $O(\text{keV})$ mass-splitting for the inelastic DM by a scalar seesaw mechanism without fine-tuning.

This paper is organized as follows. We construct our model in Sec. II. In Sec. III, we analyze the DM-electron recoil signals in various direct detection experiments. In Sec. IV, we study other laboratory constraints, including the measurements of the Z boson mass, the electron

*hjhe@sjtu.edu.cn; hjhe@tsinghua.edu.cn

†wang-yc15@mails.tsinghua.edu.cn

‡zhengjm3@sjtu.edu.cn

anomalous magnetic moment, the flavor changing processes, and the collider searches. In Sec. V, we study the cosmological constraints on our model, including the X' lifetime and the DM relic density. Finally, we conclude in Sec. VI. The Appendix A elaborates our analysis of the Higgs sector in this model.

II. GeV Scale Inelastic DM under Dark $U(1)_X$

To realize the DM-electron interaction, we extend the SM with a dark $U(1)_X$ gauge group under which both the DM and the right-handed first family fermions are charged. We also include three right-handed Majorana neutrinos ν_{Rj} ($j = 1, 2, 3$). We denote the $U(1)_X$ gauge boson (dark photon) by A'_μ . The Higgs sector consists of two Higgs doublets plus three singlet scalars S , S' and ϕ , charged under $U(1)_X$. The electroweak symmetry breaking is realized by two Higgs doublets H_1 and H_2 with vacuum expectation values (VEVs) $\langle H_j \rangle = (0, v_j)^T$ and the combined VEV is $v_h = \sqrt{v_1^2 + v_2^2} \simeq 174$ GeV. We will set $v_1^2 \ll v_2^2$, so the observed 125 GeV Higgs boson is mostly made of the CP even neutral component of H_2 . The dark $U(1)_X$ gauge group is mainly broken by the VEVs of the singlet scalars S and S' , whose VEVs $\langle S \rangle = v_S$ and $\langle S' \rangle = v_{S'}$ are of $O(100)$ GeV. Our model sets the first family fermions charged under $U(1)_X$, and the second and third family fermions as $U(1)_X$ singlets. We summarize in Table I the particle content and charge assignments of our model for the scalars and the first family fermions.

The DM particles (X, X') form a complex scalar $\hat{X} = (X + iX')/\sqrt{2}$ with $U(1)_X$ charge $q_{\hat{X}}$. As we will show, the spontaneous breaking of $U(1)_X$ can generate the desired mass-splitting Δm between X and X' . Our model builds the left-handed fermion doublets as $U(1)_X$ singlets. This forbids the decay channel $X' \rightarrow X\bar{\nu}\nu$, and thus ensures the current DM relic abundance still consists of about equal amounts of (X, X') so far. The anomaly cancellation conditions then uniquely determine the $U(1)_X$ charges of the first family fermions up to an overall normalization factor. The flavor non-universality of $U(1)_X$ is required to maintain the X' lifetime being longer than the age of our Universe, as will be shown in Sec. V.

We write down the relevant Lagrangian terms of the DM sector as follows:

$$\begin{aligned} \Delta\mathcal{L}_{\text{DM}} \supset & |D^\mu \hat{X}|^2 - m_{\hat{X}}^2 |\hat{X}|^2 - \lambda_X |\hat{X}|^4 \\ & - (\lambda_{X\phi} \hat{X}^2 \phi^2 + \text{h.c.}) - \sum_i \lambda_{X\psi_i} |\hat{X}|^2 |\psi_i|^2, \end{aligned} \quad (1)$$

where $\psi_i = H_1, H_2, S, S', \phi$. Due to the $U(1)_X$ charge assignments, the right-handed SM fermions in the first family only couple to H_1 , while the right-handed fermions in the second and third families only interact with H_2 . Thus, we can write down the Lagrangian including the relevant Yukawa terms with ν_{Rj} and the relevant poten-

Group	Q_{L1}	u_R	d_R	L_1	e_R	ν_{R1}	H_1	H_2	S	S'	ϕ	\hat{X}
$SU(2)_L$	2	1	1	2	1	1	2	2	1	1	1	1
$U(1)_Y$	$\frac{1}{6}$	$\frac{2}{3}$	$-\frac{1}{3}$	$-\frac{1}{2}$	-1	0	$\frac{1}{2}$	$\frac{1}{2}$	0	0	0	0
$U(1)_X$	0	$\frac{1}{2}$	$-\frac{1}{2}$	0	$-\frac{1}{2}$	$\frac{1}{2}$	$\frac{1}{2}$	0	-1	$\frac{1}{2}$	-3	3
\mathbb{Z}_2	$+$	$+$	$+$	$+$	$+$	$+$	$+$	$+$	$+$	$+$	$+$	$-$

TABLE I: Particle content and group assignments of the present model. Here Q_{Lj} and L_j denote the left-handed weak doublet of the SM quarks and leptons, respectively, and the subscript j is the fermion family index of the SM.

tial terms with scalar singlets:

$$\begin{aligned} \Delta\mathcal{L} \supset & \bar{e}_R i \not{D} e_R - \sum_{i=1}^3 \left(y_{i1}^\nu \bar{L}_i \tilde{H}_1 \nu_{R1} + \sum_{j=2}^3 y_{ij}^\nu \bar{L}_i \tilde{H}_2 \nu_{Rj} \right) \\ & - \frac{1}{2} \left(y_S \nu_{R1}^T S \nu_{R1} + \sum_{i,j=2}^3 M_{Rij} \nu_{Ri}^T \nu_{Rj} + \text{h.c.} \right) \\ & + M_S^2 |S|^2 + M_{S'}^2 |S'|^2 + (M'_{12} H_1^\dagger H_2 S' + \text{h.c.}) \\ & - M_\phi^2 |\phi|^2 + (\lambda_{S\phi} S^3 \phi + \text{h.c.}). \end{aligned} \quad (2)$$

We note that the cubic term $M'_{12} H_1^\dagger H_2 S'$ is needed to ensure that all the pseudoscalars are massive. In Eq.(2), the squared masses ($M_S^2, M_{S'}^2, M_\phi^2$) are all positive, so S and S' acquire VEVs from their potentials directly, whereas ϕ can only obtain a small VEV induced from $\langle S \rangle$ and $\langle S' \rangle$. In the present study, we require that the scalar potential holds the CP conservation, under which all the scalar couplings and VEVs are real. Eq.(2) shows that the singlet S and the right-handed neutrino ν_{R1} form a Yukawa interaction and generates a weak scale Majorana mass for ν_{R1} , $M_{R1} = y_{S1} v_S$. The second and third family right-handed neutrinos are $U(1)_X$ singlets, so they directly form Majorana mass terms as in Eq.(2). Thus, the light neutrino masses are generated by the type-I seesaw mechanism.

From the Lagrangian (1), we see that the DM mass is determined by the DM quadratic mass term and the DM couplings to $|H_i|^2$, $|S|^2$ and $|S'|^2$. The mass-splitting between the two DM components is determined by the unique quartic interaction $\hat{X}^2 \phi^2$ and the singlet VEV $\langle \phi \rangle$ which is naturally small as guaranteed by a scalar seesaw from the potential terms in the last line of Eq.(2). This is because ϕ is much heavier than all the other scalars and leads to $v_\phi \equiv \langle \phi \rangle \simeq \lambda_{S\phi} v_S^3 / M_\phi^2$. Thus, we derive the $X'-X$ mass-splitting:

$$\frac{m_{X'} - m_X}{m_X} \simeq \frac{\lambda_{X\phi} v_\phi^2}{m_X^2} = \frac{2\lambda_{X\phi} \lambda_{S\phi}^2 v_S^6}{m_X^2 M_\phi^4}. \quad (3)$$

Hence, to realize the desired $O(\text{keV})$ mass-splitting for explaining the XENON1T anomaly, we can choose the sample inputs, $\lambda_{X\phi}, \lambda_{S\phi} = O(0.01)$, $v_S = O(100)$ GeV,

$m_X = O(\text{GeV})$, and $M_\phi = O(\text{TeV})$, where no numerical fine-tuning is needed.

Since the Higgs doublet H_1 carries both $U(1)_Y$ and $U(1)_X$ charges, its VEV induces mass-mixing between their corresponding gauge bosons. Denoting the neutral gauge bosons of $SU(2)_L$, $U(1)_Y$ and $U(1)_X$ as $(W_\mu^3, B_\mu, \mathcal{X}_\mu)$, we derive their mass-eigenstates (Z_μ, A_μ, A'_μ) to the leading order of the gauge coupling $g_X \ll 1$ and VEV ratio $v_1^2/v_h^2 \ll 1$. Thus, we compute their mass-eigenvalues,

$$\begin{aligned} m_A^2 &= 0, \\ m_{A'}^2 &\simeq 2g_X^2 \left(v_S^2 + \frac{1}{4}v_{S'}^2 \right), \\ m_Z^2 &\simeq \frac{1}{2} \left(g^2 + g'^2 + g_X^2 \frac{v_1^4}{v_h^4} \right) v_h^2, \end{aligned} \quad (4)$$

and their mixing matrix to the leading order,

$$\begin{pmatrix} A'_\mu \\ A_\mu \\ Z_\mu \end{pmatrix} = \begin{pmatrix} 1 & \frac{-g'g_X}{g^2+g'^2} \frac{v_1^2}{v_h^2} & \frac{gg_X}{g^2+g'^2} \frac{v_1^2}{v_h^2} \\ 0 & \frac{g}{\sqrt{g^2+g'^2}} & \frac{g'}{\sqrt{g^2+g'^2}} \\ \frac{-g_X}{\sqrt{g^2+g'^2}} \frac{v_1^2}{v_h^2} & \frac{-g'}{\sqrt{g^2+g'^2}} & \frac{g}{\sqrt{g^2+g'^2}} \end{pmatrix} \begin{pmatrix} \mathcal{X}_\mu \\ B_\mu \\ W_\mu^3 \end{pmatrix}. \quad (5)$$

III. Analyzing Constraints of DM Direct Detections

In the present model, we derive the DM-electron inelastic scattering cross section with zero-momentum-transfer:

$$\bar{\sigma}_e \equiv \sigma_{Xe}(|\mathbf{q}|=0) = \frac{q_e^2 q_{\hat{X}}^2 g_X^4}{4\pi} \frac{m_e^2}{m_{A'}^4}, \quad (6)$$

where e_R and \hat{X} carry the $U(1)_X$ charges $q_e = -\frac{1}{2}$ and $q_{\hat{X}} = 3$, respectively. In Ref. [8], using the effective field theory (EFT) approach we did a model-independent fit of the inelastic DM for the electron recoil spectrum in the XENON1T detection [2]. We showed that the observed event excess by XENON1T [1] can be fully explained from the two-component inelastic DM with mass-spitting $\Delta m \equiv m_{X'} - m_X = (2-3) \text{ keV}$, and the typical DM-electron inelastic scattering cross section is $\bar{\sigma}_e/m_X = (8.8 \pm 4.0) \times 10^{-44} \text{ cm}^2/\text{GeV}$, for the inelastic DM containing equal amount of X and X' particles. Thus, by fitting the XENON1T data [1], we derive the following constraint on the current model:

$$\frac{m_{A'}}{g_X} = 1.2^{+0.2}_{-0.1} \times 10^2 \text{ GeV} \times \left[\left| \frac{q_e q_{\hat{X}}}{3/2} \right|^{\frac{1}{2}} \left(\frac{1 \text{ GeV}}{m_X} \right)^{\frac{1}{4}} \right]. \quad (7)$$

In Fig. 1, we show $m_{A'}/g_X$ as a function of the DM mass m_X . By fitting the recent XENON1T data [1], we plot the central values by red solid curve and depict the allowed parameter space by the red shaded area at 95% C.L.

PandaX-II collaboration has accumulated 100.7 ton-day data from measuring the electron recoil event rate [3].

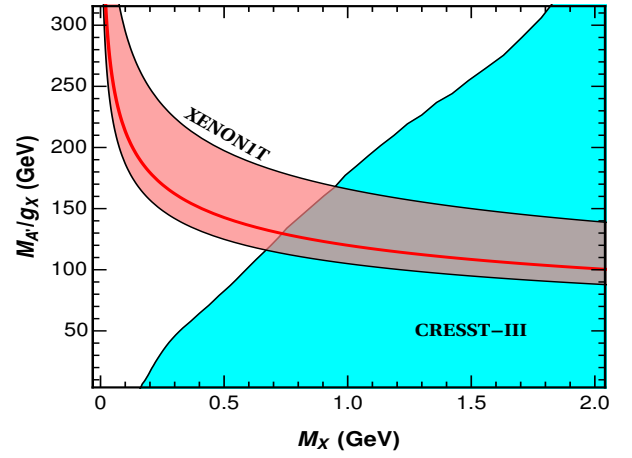


FIG. 1: Constraints on our model by the direct DM detections of XENON1T and CRESST-III. The red solid curve shows the central value and the red shaded area gives the allowed region (95% C.L.) from fitting the electron recoil data of XENON1T [1]. The blue shaded region is excluded by the nucleus recoil detection of CRESST-III at 90% C.L. [12].

In each bin of the PandaX-II data, we fit the expected DM signals to be less than 10 events/keV, which is smaller than the error bar. Hence, we conclude that the best fit of our model is consistent with PandaX-II although its current bound is too weak to be shown in Fig. 1.

The DM particles of our model can also scatter with nucleus by exchanging the mediator particle A'_μ since the quarks (u_R, d_R) carry $U(1)_X$ charges as in Table I. The DM-nucleus scattering is dominated by the spin-independent interaction as induced by the mediator couplings with the DM and quarks. To compare with the results from nuclear recoil detection experiments, we compute the DM-nucleon scattering cross section as follows [10, 11],

$$\sigma_{XN} = \frac{m_N^2 m_X^2 q_{\hat{X}}^2}{16\pi(m_X + m_N)^2 m_{A'}^4}, \quad (8)$$

where $m_N \simeq 940 \text{ MeV}$ is the mass of nucleons. We find that for the GeV scale DM, the strongest constraint is set by the direct detection experiment CRESST-III [12], which can achieve a nuclear recoil threshold energy as low as 30.1 eV and thus rather sensitive to the light DM of mass below $\sim 2 \text{ GeV}$. In Fig. 1, we present the CRESST-III bound (90% C.L.) on the parameter space of our model as the blue shaded region.¹ This constrains the mass of the inelastic DM as $m_X \lesssim 1 \text{ GeV}$.

¹ Note that for DM mass $\lesssim 1 \text{ GeV}$, the typical recoil energy of scattering off an oxygen or tungsten nucleus is below keV. We thus only include the down scattering process $X' + N \rightarrow X + N$ for the bound.

IV. Analyzing Laboratory Constraints

In this section, we proceed to analyze the relevant laboratory constraints on our model.

► *Correction to Z Boson Mass*

Our model contributes to several electroweak precision observables. Using Eq.(4), we derive the new correction to Z boson mass:

$$\delta m_Z = \frac{g_X^2 v_1^4}{4v_h^2 m_Z}. \quad (9)$$

The Z pole observables have been measured with high precision. Especially, the SM prediction gives $m_Z^{\text{sm}} = (91.1884 \pm 0.0020)$ GeV and the measured value is $m_Z^{\text{exp}} = (91.1876 \pm 0.0021)$ GeV [13]. This strongly constrains any new physics contribution to the Z boson mass, $\delta m_Z < 0.0049$ GeV at 95% C.L. This constrains the VEV of the Higgs doublet H_1 ,

$$v_1 \lesssim 15.2 \text{ GeV} / \sqrt{g_X}. \quad (10)$$

► *Correction to Electron Anomalous Magnetic Moment*

The $U(1)_X$ interaction also alters the anomalous magnetic moments of electrons. For $m_{A'} \gg m_e$, the one-loop correction to $a_e = \frac{1}{2}(g_e - 2)$ can be derived:

$$\delta a_e^X \simeq -\frac{g_X^2 q_e^2}{12\pi^2} \frac{m_e^2}{m_{A'}^2}, \quad (11)$$

with $q_e = -\frac{1}{2}$, which agrees with [14]. For $(g_X, m_{A'})$ satisfying Eq.(7), and $q_{\hat{X}} = 3$, we derive the correction to the electron anomalous magnetic moment, $\delta a_e^X \simeq 4 \times 10^{-14}$, which is lower than the current experiment sensitivity of 10^{-13} [13].

► *Other Constraints on the Higgs Sector*

There are additional bounds that can constrain the Higgs sector of our model. For instance, the signal strength of the SM-like Higgs boson $h(125\text{GeV})$ measured at the LHC can constrain the mixing between the CP-even neutral component of H_2 and the other scalar singlets. The flavor specific nature of our two-Higgs-doublet sector generally leads to flavor-changing processes induced by the Higgs-exchange, so the mass of the heavy neutral Higgs (mainly from H_1 doublet) is constrained by meson mixings. Since the present study focuses on analyzing the DM and its vector portal to the SM particles, we will present these constraints on the Higgs sector in Appendix A.

► *Collider Constraints*

Since the mediator A'_μ couples directly to the right-handed electrons, our model will receive nontrivial constraints from e^+e^- colliders. (There are discussions on constraining light DM models at lepton colliders in the literature [15–17].) The mediator A'_μ contributes constructively to the cross section of the scattering process

$e^+e^- \rightarrow e^+e^-$. Its cross section has been measured by LEP [18], with which we infer a bound on our model, $\sqrt{4\pi s}/(q_e g_X) > 8.6 \text{ TeV}$ at 95% C.L.,² where $\sqrt{s} \simeq 200$ GeV is the LEP collider energy. Thus, for $q_e = -\frac{1}{2}$ in our model, this imposes a bound on the gauge coupling, $g_X \lesssim 0.164$.

The DM particles can be pair-produced in e^+e^- collisions through s -channel $A'(Z)$ -exchanges and in association with the final state mono-photon, $e^+e^- \rightarrow XX'\gamma$. The rate of the DM production with mono-photon via Z -exchange is highly suppressed by a coupling factor v_1^4/v_h^4 which arises from the gauge boson mixing matrix (5). As we will show in Sec.V and Fig.2, the A' mass has to be less than a few GeV due to the combined bounds of realizing the DM relic density and fitting the XENON1T data. We find that for the A'_μ contribution in the case of $\sqrt{s} > m_{A'} > 2m_X$ at LEP [19], the cross section of this process has a resonance at $E_\gamma/E_{\text{beam}} \sim 1 - m_{A'}^2/s$. The bound from this resonance together with XENON1T and DM relic density constrains the gauge coupling $g_X \lesssim 0.001$ and $m_{A'} \lesssim 0.3 \text{ GeV}$. We also find that the $m_{A'} < 2m_X$ region obeying the DM relic density bound is always allowed by the LEP mono-photon searches. The mono-photon searches at low energy e^+e^- colliders such as BaBar [20] and Belle-II [21] can also place non-trivial bounds on models of light dark matter [16]. For the mass ranges $m_X \lesssim 1 \text{ GeV}$ and $m_{A'} \lesssim 2m_X$, the BaBar measurements constrain $g_X^2 q_e q_{\hat{X}} < O(10^{-2})$. For the ongoing Belle-II experiment, the prospective constraint set by null result is $g_X^2 q_e q_{\hat{X}} < O(10^{-3})$, by assuming ideally that the backgrounds are perfectly known. As we will discuss in Sec. V, combining the constraints from the XENON1T data, the CRESST-III data, and realizing the DM relic abundance will require $g_X \lesssim 0.018$ and satisfy the LEP collider bounds.

The LHC measurement of $Z \rightarrow 4\mu$ decays [22] can constrain the coupling between A'_μ and μ^\pm . This coupling is induced from the neutral gauge boson mixings in Eq.(5),

$$\mathcal{L} \supset g_X \frac{v_1^2}{v_h^2} \bar{\mu} \left[\left(\sin^2 \theta_W - \frac{1}{4} \right) \gamma^\mu - \frac{1}{4} \gamma^5 \gamma^\mu \right] A'_\mu \mu. \quad (12)$$

For the vector-type interaction with a small mediator mass $m_{A'} < 10 \text{ GeV}$, we find that the LHC has placed a bound on the new coupling $g_{\text{new}} \lesssim 4.5 \times 10^{-3}$ at 95% C.L. For $v_1^2/v_h^2 = 10^{-2}$, we convert the LHC bound to our model and deduce $g_X \lesssim O(1)$, which is weaker than the LEP bound of fermion-pair productions. The DM particles can also be directly produced at the LHC due to its coupling to the right-handed quarks (u_R, d_R), giving raise to mono-photon signals together with missing E_T . Such signals have been actively searched at ATLAS [23] and CMS [24]. But, these searches lose sensitivity for

² Hereafter all the quoted experimental bounds are set at 95% C.L. unless specified otherwise.

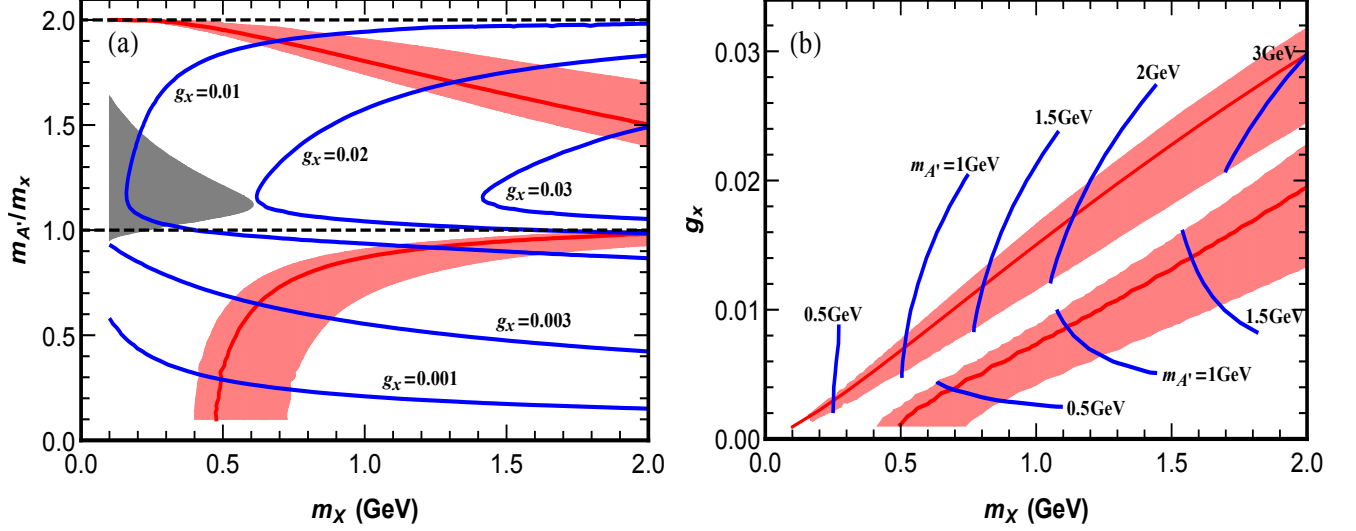


FIG. 2: Plot (a): Constraints on the parameter space of m_X versus $m_{A'}/m_X$. The blue curves show the parameter space of realizing the observed DM relic abundance for a set of sample values of g_X . Plot (b): Constraints on the parameter space of m_X versus g_X . The blue curves show the parameter space of realizing the observed DM relic abundance for a set of sample mediator masses $m_{A'}$. In each plot, the shaded pink areas depict the allowed regions (95% C.L.) by the XENON1T data combined with the DM relic density bound, and the red solid curve denotes the best-fit values.

$g_X < O(0.1)$ [25] and does not constrain the cosmologically favored parameter space as we will discuss in Sec. V.

V. Analyzing Cosmological Constraints

In this section, we analyze the relevant cosmological constraints on the present inelastic DM model.

► Lifetime of the Heavier DM X'

To resolve the XENON1T anomaly by inelastic DM, it is important to ensure the lifetime of the heavier DM component X' being longer than the age of the Universe. Since we have the DM mass-splitting $\Delta m \ll m_e$, only the decays such as $X' \rightarrow X\gamma\gamma$ and $X' \rightarrow X\nu\bar{\nu}$ are kinematically allowed. The former occurs through one-loop diagrams with electron running in the loop. Thus, with [8, 26], we can estimate the decay width of X' as

$$\Gamma_{X' \rightarrow X\gamma\gamma} \simeq \frac{\alpha^2 g_X^4 q_e^2 q_{\hat{X}}^2}{7560\pi^5} \frac{\Delta m^9}{m_e^4 m_{A'}^4}. \quad (13)$$

From fitting the XENON1T event rate, we have a small DM mass-splitting $\Delta m \simeq 3 \text{ keV}$ and the ratio of $m_{A'}/g_X$ given by Eq.(7). This leads to tiny partial decay rate $\Gamma_{X' \rightarrow X\gamma\gamma} \approx 1/(3 \times 10^{23} \text{ yr})$ and thus $\Gamma_{X' \rightarrow X\gamma\gamma}^{-1} \gg \tau_U$, where $\tau_U \simeq 1.38 \times 10^{10} \text{ yr}$ is the age of the Universe.

The other decay channel $X' \rightarrow X\nu\bar{\nu}$ occurs through the A' - Z mixing in Eq.(5). Thus, we can estimate X' decay width as follows:

$$\Gamma_{X' \rightarrow X\nu\bar{\nu}} \simeq \frac{g'^2 g_X^4 q_{\hat{X}}^2}{480\pi^3} \frac{v_1^4 \Delta m^5}{m_Z^4 m_{A'}^4}. \quad (14)$$

Requiring $\Gamma_{X' \rightarrow X\nu\bar{\nu}} \lesssim \tau_U^{-1}$, we derive the following constraint:

$$v_1 \lesssim 40 \text{ GeV} \times \left(\frac{1 \text{ GeV}}{m_X} \right)^{\frac{1}{4}}. \quad (15)$$

This shows that in our model the electroweak symmetry breaking (EWSB) is mainly generated by the Higgs doublet H_2 , and the VEV ratio $\tan \beta = v_2/v_1 \gtrsim 4$.

► DM Relic Abundance

Since our construction always holds $\Delta m \ll m_X$, the DM components can be regarded as a degenerate complex scalar before their freeze-out. We thus determine the relic density of a complex scalar \hat{X} . The correct DM relic density can be achieved in the DM freeze-out scenario for two distinctive regimes of the parameter space. The dominant annihilation process during the freeze-out is either $\hat{X}\hat{X}^* \rightarrow A'A'$ for $m_X > m_{A'}$, or, the resonance process $\hat{X}\hat{X}^* \rightarrow A'$ for $m_{A'} \approx 2m_X$. We compute the DM relic density of the current model with the code `MicrOMEGAs` [10, 27] and present our results in Fig. 2. In the left panel, the blue curves show the masses of A' and X (X') which achieve the observed relic DM abundance, for each given value of the gauge coupling g_X . The shaded pink areas present the allowed regions (95% C.L.) by the XENON1T data combined with the DM relic density bound, and the red solid curves denote the best-fit values. The region of $m_{A'}/m_X > 2$ is mostly excluded by LEP mono-photon constraints, as discussed in Sec. IV. The pink regions in the right panel show the allowed parameter space of m_X versus g_X at 95% C.L. For each given mediator mass $m_{A'}$, the observed

DM relic abundance can be achieved by two distinct solutions of g_X , which is also evident in the left panel. The upper pink shaded band corresponds to the region of $1 < m_{A'}/m_X < 2$, whereas the lower pink band corresponds to the region of $m_{A'}/m_X < 1$. The blue curves show the allowed value of the gauge coupling g_X as a function of the DM mass m_X , which achieves the observed DM relic abundance for each given value of the mediator mass $m_{A'}$. We fit the XENON1T data and relic density bound together, and include CRESST-III constraint of $m_X \lesssim 1$ GeV (Fig. 1). With these, we derive the combined limit $g_X \lesssim 0.018$, which is stronger than the collider bounds.

► Current Ratio of X and X'

Finally, we examine whether the constrained couplings in Fig. 2(b) are consistent with the assumption of $n_X = n_{X'}$. After the decoupling of the annihilation process $\hat{X}\hat{X}^* \rightarrow A'A'$, the total DM number density $n_{\hat{X}} = n_X + n_{X'}$ is fixed. However, X and X' can still convert to each other through the processes $e^\pm X \leftrightarrow e^\pm X'$ and $X'X' \leftrightarrow XX$. As we showed in [8], the former process decouples when $T \sim m_e \gg \Delta m$ for GeV scale DM with electron scattering cross-section satisfying the XENON1T signal rate. The latter process is induced by t - and u -channel exchanges of A' . If the annihilation $X'X' \rightarrow XX$ decouples at a temperature $T' < \Delta m$, the X' density would be exponentially suppressed by a factor of $\exp(-\Delta m/T')$. As an estimate, this process becomes inefficient when $\Gamma(T') \lesssim H(T')$. The reaction rate is estimated as $\Gamma(T') \simeq \langle \sigma' v_{\text{DM}} \rangle n_{\text{DM}}$, with the thermally averaged DM annihilation cross section $\langle \sigma' v_{\text{DM}} \rangle \simeq \tilde{g}_X^4 \sqrt{m_X^3 T'} / (\pi m_{A'}^4)$ and the DM density $n_{\text{DM}} \simeq T_{\text{eq}} T'^3 / m_X$. Here T_{eq} is the temperature at the matter-radiation equality. Thus, we can estimate

$$T' \simeq 5 \text{ MeV} \times \left(\frac{0.05}{g_X} \right)^{\frac{8}{3}} \left(\frac{m_{A'}}{5 \text{ GeV}} \right)^{\frac{8}{3}} \left(\frac{3 \text{ GeV}}{m_X} \right)^{\frac{1}{3}}. \quad (16)$$

Shortly after the kinetic decoupling, the temperature of the DM drops rapidly as $a(t)^{-2}$ and falls below Δm quickly. The X' density would get depleted if the annihilation $X'X' \rightarrow XX$ is still efficient. As a conservative estimate, we demand $T' \gtrsim m_e$, so the process $X'X' \rightarrow XX$ decouples before the kinetic decoupling between e^\pm and the DM. This constraint excludes the gray shaded region in the left panel of Fig. 2, and is satisfied by the parameter space as allowed by both the XENON1T event rate and the DM relic abundance.

VI. Conclusions

In this work, we proposed a new candidate of GeV scale inelastic dark matter (DM). For this we constructed a renormalizable inelastic DM model under extra $U(1)_X$ gauge symmetry with a GeV scale dark photon mediator (cf. Table I). We realized the natural $O(\text{keV})$ mass-splitting for the inelastic DM by a scalar seesaw mecha-

nism without fine-tuning. Our model is highly testable and we derived nontrivial experimental bounds, including those by the DM relic abundance, the lifetime of the heavier DM component, the collider searches, and the electroweak precision tests. Under these constraints, we resolved the recent XENON1T anomaly [2] via electron recoil detection, and predicted the inelastic DM with mass $\lesssim 1$ GeV, as shown in Fig. 1-2. We further derived new limits on our inelastic DM via the nuclear recoil detection by the CRESST-III experiment. This is combined with our fit of the XENON1T data to identify the viable parameter space of our model in Fig. 1. The upcoming DM direct detection measurements by PandaX-4T [29], LZ [30], and XENONnT [31] will provide decisive probes of our GeV scale inelastic DM candidate.

Acknowledgements

This research was supported in part by the National NSF of China (under grants 11675086 and 11835005), by the CAS Center for Excellence in Particle Physics (CCEPP), and by the National Key R&D Program of China (No.2017YFA0402204). It was also supported in part by the Key Laboratory for Particle Physics, Astrophysics and Cosmology (MoE) and by the Office of Science and Technology, Shanghai Municipal Government (No. 16DZ2260200).

A. Constraints on the Higgs Sector

In this Appendix, we present the constraints on the Higgs sector of our model. For convenience, we denote the CP even neutral components of H_1 , H_2 , and S' as h_1 , h_2 and $h_{S'}$, respectively. We consider the case of $M_{h_1}^2 \gg M_{h_2}^2$ and $v_1^2 \ll v_2^2$, and thus the observed 125 GeV Higgs boson h mainly contains the h_2 state. To realize these conditions, we consider the relevant part of the scalar potential,

$$V \supset M_{H_1}^2 |H_1|^2 - M_{H_2}^2 |H_2|^2 - M_{S'}^2 |S'|^2 - M' H_1^\dagger H_2 S' + \lambda_1 |H_1|^4 + \lambda_2 |H_2|^4 + \lambda_3 |H_1|^2 |H_2|^2 + \lambda_{S'} |S'|^4 + \lambda_{H_1 S'} |H_1|^2 |S'|^2 + \lambda_{H_2 S'} |H_2|^2 |S'|^2, \quad (A1)$$

where we only list terms relevant to H_1 , H_2 and S' . The cubic term $H_1^\dagger H_2 S'$ will ensure nonzero mass of the pseudoscalars. In Eq.(A1), we take all the mass parameters and the quartic couplings be positive. We choose the Higgs doublet H_1 with a large positive mass term with $M_{H_1}^2 \gg v_2^2, v_{S'}^2$. Thus, we deduce the VEV of H_1 ,

$$v_1 \simeq \frac{v_2 v_{S'} M'}{M_{H_1}^2}. \quad (A2)$$

We see that requiring $M_{H_1}^2 \gg M' v_{S'}$ can realize $v_1^2 \ll v_2^2$. ATLAS and CMS have measured the signal strength of the Higgs boson h (125 GeV) for various channels, defined

as $\mu_h \equiv \langle \sigma_h \cdot \text{BR} \rangle_{\text{obs}} / \langle \sigma_h \cdot \text{BR} \rangle_{\text{SM}}$, with σ_h the h production cross section and BR the decay branching fraction of a given channel. The most precisely measured channels are $\gamma\gamma$ and WW^* which are consistent with the SM ($\mu_h = 1$) to 10% level [13]. This constrains the mixing of the SM-like Higgs boson h_2 with $h_{S'}$ and h_1 down to 10% level. Note that for $v_1^2 \ll v_2^2$, the h_2 - h_1 mixing is mainly generated by the cubic term $-M'H_1^\dagger H_2 S'$, and the contributions from the mixed quartic terms are suppressed by v_1 . Thus, for $M_{H_1}^2 \gg M_{H_2}^2$, the h_2 - h_1 mixing is mainly determined by $|M'v_{S'}/M_{H_1}^2| \simeq v_1/v_2$. With this condition, we may choose the VEV ratio

$$v_1/v_2 \lesssim 0.1. \quad (\text{A3})$$

The small h_2 - $h_{S'}$ mixing can be induced by the contributions from the cubic and quartic terms with opposite signs. As an estimate, we ignore the small mixing of the heavy h_1 with the lighter states h_2 or $h_{S'}$ and obtain,

$$|\sin \theta_{h_2 h_{S'}}| \simeq \left| \frac{\lambda_{H_2 S'} v_2 v_{S'} - M' v_1}{M_h^2 - M_{h_{S'}}^2} \right| \ll 1. \quad (\text{A4})$$

Another constraint on the heavy Higgs mass M_{H_1} comes from the flavor-changing processes mediated by the heavy scalars. The general Yukawa interactions for the quark sector take the following form,

$$\begin{aligned} \mathcal{L} = & - \sum_{i=1}^3 \left(y_u^{i1} \bar{Q}_{Li} \tilde{H}_1 u_{R1} + y_d^{i1} \bar{Q}_{Li} H_1 d_{R1} \right) \\ & - \sum_{i=1,2,3}^{j=2,3} \left(y_u^{ij} \bar{Q}_{Li} \tilde{H}_2 u_{Rj} + y_d^{ij} \bar{Q}_{Li} H_2 d_{Rj} \right) \\ \equiv & - \bar{Q}_L^i \left(\tilde{\mathbf{y}}_u \tilde{H}_1, \hat{\mathbf{y}}_u \tilde{H}_2 \right)_{ij} u_{Rj} - \bar{Q}_L^i \left(\tilde{\mathbf{y}}_d H_1, \hat{\mathbf{y}}_d H_2 \right)_{ij} d_{Rj} \end{aligned} \quad (\text{A5a})$$

$$(\text{A5b})$$

where we denote $\tilde{H}_i = i\sigma_2 H_i^*$. For convenience, in the last line, we have decomposed the 3×3 Yukawa matrix $\mathbf{y}^{u,d} = (\tilde{\mathbf{y}}_{u,d}, \hat{\mathbf{y}}_{u,d})_{ij}$. Here, $\tilde{\mathbf{y}}_{u,d}$ are 3×1 matrices of Yukawa couplings to H_1 and $\hat{\mathbf{y}}_{u,d}$ are 3×2 matrices of Yukawa couplings to H_2 . The quarks acquire masses via Yukawa interactions with H_1 and H_2 taking their VEVs. The mass eigenstates are obtained by chiral rotations,

$$\mathbf{u}'_L = U_L^u \mathbf{u}_L, \quad \mathbf{d}'_L = U_L^d \mathbf{d}_L, \quad (\text{A6a})$$

$$\mathbf{u}'_R = U_R^{u\dagger} \mathbf{u}_R, \quad \mathbf{d}'_R = U_R^{d\dagger} \mathbf{d}_R, \quad (\text{A6b})$$

where \mathbf{u} and \mathbf{d} are vectors in flavor space denoting the 3 family of quarks, and $U_{L,R}^{u,d}$ are unitary rotation matrices. The quark mass matrices are diagonalized as

$$U_L^{u\dagger} \left(\tilde{\mathbf{y}}_u v_1, \hat{\mathbf{y}}_u v_2 \right) U_R^u = v_2 \mathbf{y}_u^{\text{diag}}, \quad (\text{A7a})$$

$$U_L^{d\dagger} \left(\tilde{\mathbf{y}}_d v_1, \hat{\mathbf{y}}_d v_2 \right) U_R^d = v_2 \mathbf{y}_d^{\text{diag}}, \quad (\text{A7b})$$

where $v_2 \mathbf{y}_{u(d)}^{\text{diag}}$ is the 3×3 diagonal mass matrix for up-type (down-type) quarks, whose diagonal elements equal to the SM quark masses (in the limit of $v_1 \ll v_2$). In the mass-eigenbasis, the Yukawa interactions for the up-type quarks become:

$$\mathcal{L} = -\bar{\mathbf{u}}'_L U_L^{u\dagger} \left(\tilde{\mathbf{y}}_u \tilde{H}_1, \hat{\mathbf{y}}_u \tilde{H}_2 \right) U_R^u \mathbf{u}'_R \quad (\text{A8a})$$

$$\begin{aligned} = & -\bar{\mathbf{u}}'_L U_L^{u\dagger} \left(\tilde{\mathbf{y}}_u \left(\tilde{H}_1 - \frac{v_1}{v_2} \tilde{H}_2 \right), (\mathbf{0}) \right) U_R^u \mathbf{u}'_R \\ & - \bar{\mathbf{u}}'_L \mathbf{y}_u^{\text{diag}} \tilde{H}_2 \mathbf{u}'_R, \end{aligned} \quad (\text{A8b})$$

and similarly for down-type quarks under the replacement $\mathbf{u} \rightarrow \mathbf{d}$ and $\tilde{H}_i \rightarrow H_i$. In the above, $(\mathbf{0})$ denotes a 3×2 matrix with all elements vanishing. The first term in Eq.(A8b) would induce flavor-changing processes if the flavor mixing matrices $U_{L,R}^u$ take arbitrary pattern, and in this case it will receive strong constraints by the meson mixings. It is known that for well-motivated scenarios of flavor mixing such constraints can be much reduced. For instance, we may consider Cheng-Sher-like ansatz [32] on the flavor-changing Yukawa couplings,

$$\xi_{u,d}^{ij} = O \left(\sqrt{m_{u,d}^i m_{u,d}^j} / v_h \right), \quad (\text{A9})$$

where (i, j) are family indices. Thus, we set

$$U_L^{u,d\dagger} \left(\tilde{\mathbf{y}}_{u,d}, (\mathbf{0}) \right) U_R^{u,d} = \xi_{u,d}. \quad (\text{A10})$$

Then, the flavor-changing process between the i -th and j -th families is characterized by the new physics (NP) scale,

$$\Lambda_{\text{NP}} = \min \left(M_{H_1}, \frac{v_2}{v_1} M_h \right) v_h / \sqrt{m_{u,d}^i m_{u,d}^j}. \quad (\text{A11})$$

For instance, the measurements of K - \bar{K} mixing constrain $\Lambda_{\text{NP}} \gtrsim 10^5 \text{ TeV}$ [28]. This in turn requires $M_{H_1} \gtrsim 12 \text{ TeV}$ and $v_1 \lesssim 1.7 \text{ GeV}$. The $U(1)_X$ gauge boson A'_μ also mediates flavor-violating process since it only couples to the right-handed quarks and leptons in the first family. The ratio $m_{A'}/g_X$ is constrained by fitting the XENON1T data as in Eq.(7). The meson mixing measurements will require the right-handed mass-eigenstates u'_R and d'_R to be mainly aligned with the gauge eigenstates u_R and d_R . Also, we note that similar flavor violating effects can also occur in the lepton sector and induces flavor-violating leptonic decay channel of the light Higgs boson h (125 GeV). For instance, this leads to the interesting decay channel $h \rightarrow \mu^\pm e^\mp$, which can be searched at the LHC Run-2 [33]. The upcoming LHC Run-3 and HL-LHC runs will have strong potential to discover this channel.

-
- [1] E. Aprile *et al.* [XENON Collaboration], “Energy resolution and linearity in the keV to MeV range measured in XENON1T”, *Eur. Phys. J. C* 80 (2020) 785, no.8 [arXiv:2003.03825 [physics.ins-det]].
- [2] E. Aprile *et al.* [XENON Collaboration], “Observation of Excess Electronic Recoil Events in XENON1T”, *Phys. Rev. D* 102 (2020) 072004, no.7, [arXiv:2006.09721 [hep-ex]].
- [3] X. Zhou *et al.* [PandaX-II Collaboration], “A search for solar axions and anomalous neutrino magnetic moment with the complete PandaX-II data”, arXiv:2008.06485 [hep-ex].
- [4] A. E. Robinson, arXiv:2006.13278 [hep-ex].
- [5] K. Kannike, M. Raidal, H. Veermae, A. Strumia, and D. Teresi, “Dark Matter and the XENON1T electron recoil excess”, *Phys. Rev. D* 102 (2020) 095002, no.9 [arXiv:2006.10735 [hep-ph]].
- [6] L. Di Luzio, M. Fedele, M. Giannotti, F. Mescia and E. Nardi, arXiv:2006.12487 [hep-ph]. F. Takahashi, M. Yamada and W. Yin, arXiv:2006.10035 [hep-ph]; G. Alonso-Alvarez, F. Ertas, J. Jaeckel, F. Kahlhoefer, and L. J. and Thormaehlen, arXiv:2006.11243 [hep-ph]; C. Boehm, D. G. Cerdeno, M. Fairbairn, P. A. N. Machado, and A. C. Vincent, arXiv:2006.11250 [hep-ph]; D. A. Sierra, V. DeRomeri, L. J. Flores, and D. K. Papoulias, arXiv:2006.12457 [hep-ph]; B. Fornal, P. Sandick, J. Shu, M. Su, and Y. Zhao, arXiv:2006.11264 [hep-ph]; L. Su, W. Wang, L. Wu, J. M. Yang and B. Zhu, arXiv:2006.11837 [hep-ph]; Y. Chen, J. Shu, X. Xue, G. Yuan, and Q. Yuan, arXiv:2006.12447 [hep-ph]; Q. H. Cao, R. Ding, and Q. F. Xiang, arXiv:2006.12767 [hep-ph]; H. Alhazmi, D. Kim, K. Kong, G. Mohlabeng, J. C. Park and S. Shin, arXiv:2006.16252 [hep-ph]; Y. Jho, J. C. Park, S. C. Park, and P. Y. Tseng, arXiv:2006.13910 [hep-ph]; S. Chigusa, M. Endo and K. Kohri, arXiv:2007.01663 [hep-ph]. J. Smirnov and J. F. Beacom, arXiv:2002.04038 [hep-ph]; A. Bally, S. Jana, and A. Trautner, arXiv:2006.11919 [hep-ph]; M. Du, J. Liang, Z. Liu, V. Q. Tran, and Y. Xue, arXiv:2006.11949 [hep-ph]; D. Aristizabal Sierra, V. De Romeri, L. J. Flores, and D. K. Papoulias, arXiv:2006.12457 [hep-ph]; N. F. Bell, J. B. Dent, B. Dutta, S. Ghosh, J. Kumar, and J. L. Newstead, arXiv:2006.12461 [hep-ph]; G. Paz, A. A. Petrov, M. Tamaro, and J. Zupan, arXiv:2006.12462 [hep-ph]; J. Buch, M. A. Buen-Abad, J. Fan, and J. S. C. Leung, arXiv:2006.12488 [hep-ph]; K. U. Dey, T. N. Maity, and T. S. Ray, arXiv:2006.12529 [hep-ph]; A. N. Khan, arXiv:2006.12887 [hep-ph]; K. Nakayama and Y. Tang, arXiv:2006.13159 [hep-ph]; L. Zu, G. W. Yuan, L. Feng and Y. Z. Fan, arXiv:2006.14577 [hep-ph]; M. Lindner, Y. Mambrini, T. B. Melo, and F. S. Queiroz, arXiv:2006.14590 [hep-ph]. W. DeRocco, P. W. Graham, S. Rajendran, arXiv:2006.15112 [hep-ph]; M. Chala and A. Titov, arXiv:2006.14596 [hep-ph]; C. Gao, J. Liu, L. T. Wang, X. P. Wang, W. Xue, and Y. M. Zhong, arXiv:2006.14598 [hep-ph]; J. B. Dent, B. Dutta, J. L. Newstead, and A. Thompson, arXiv:2006.15118 [hep-ph]; P. Ko and Y. Tang, arXiv:2006.15822 [hep-ph]; W. Chao, Y. Gao, and M. Jin, arXiv:2006.16145 [hep-ph]; L. Delle Rose, G. Hütsi, C. Marzo, and L. Marzola, arXiv:2006.16078 [hep-ph]; B. Bhattacharjee and R. Sengupta, arXiv:2006.16172 [hep-ph]; Y. Gao and T. Li, arXiv:2006.16192 [hep-ph]; M. Szydagis, C. Levy, G. M. Blockinger, A. Kamaha, N. Parveen and G. R. C. Rischbieter, arXiv:2007.00528 [hep-ex]; T. Li, arXiv:2007.00874 [hep-ph]; O. G. Miranda, D. K. Papoulias, M. Tortola, and J. W. F. Valle, arXiv:2007.01765 [hep-ph]; K. Benakli, C. Branchina and G. Lafforgue-Marmet, arXiv:2007.02655 [hep-ph]; N. Okada, S. Okada, D. Raut, and Q. Shafi, arXiv:2007.02898 [hep-ph]; J. Davighi, M. McCullough, and J. Tooby-Smith, arXiv:2007.03662 [hep-ph]; P. Athron, *et al.*, arXiv:2007.05517 [astro-ph.CO]; G. Arcadi, A. Bally, F. Goertz, K. Tame-Narvaez, V. Tenorth and S. Vogl, arXiv:2007.08500 [hep-ph]; C. Han, M. L. López-Ibañez, A. Melis, O. Vives and J. M. Yang, arXiv:2007.08834 [hep-ph]; Y. Ema, F. Sala and R. Sato, arXiv:2007.09105 [hep-ph]; J. Kim, T. Nomura and H. Okada, arXiv:2007.09894 [hep-ph]; J. Cao, X. Du, Z. Li, F. Wang and Y. Zhang, arXiv:2007.09981 [hep-ph]; D. Borah, S. Mahapatra, D. Nanda and N. Sahu, arXiv:2007.10754 [hep-ph]. S. Karmakar and S. Pandey, arXiv:2007.11892 [hep-ph]; S. Khan, arXiv:2007.13008 [hep-ph]; S. Shakeri, F. Hajkarim, and S. S. Xue, arXiv:2008.05029 [hep-ph]; R. G. Cai, S. Sun, B. Zhang, and Y. L. Zhang, arXiv:2009.02315 [hep-ph]; R. Foot, arXiv:2011.02590 [hep-ph]. Y. Farzan and M. Rajaei, arXiv:2007.14421 [hep-ph].
- [7] K. Harigaya, Y. Nakai and M. Suzuki, arXiv:2006.11938 [hep-ph]; H. M. Lee, arXiv: 2006.13183 [hep-ph]; M. Baryakhtar, A. Berlin, H. Liu and N. Weiner, arXiv:2006.13918 [hep-ph]; J. Bramante and N. Song, arXiv:2006.14089 [hep-ph]; I. M. Bloch, A. Caputo, R. Essig, D. Redigolo, M. Sholapurkar, and T. Volansky, arXiv:2006.14521 [hep-ph]; H. An and D. Yang, arXiv:2006. 15672 [hep-ph]; S. Baek, J. Kim, and P. Ko, arXiv:2006. 16876 [hep-ph]; A. Aboubrahim, M. Klasen and P. Nath, arXiv:2011.08053 [hep-ph].
- [8] H. J. He, Y. C. Wang, and J. Zheng, *JCAP* (2020), in press [arXiv:2007.04963].
- [9] For a review of the 2HDM, G. C. Branco, P. M. Ferreira, L. Lavoura, M. N. Rebelo, M. Sher and J. P. Silva, *Phys. Rept.* 516 (2012) 1 [arXiv:1106.0034 [hep-ph]]; and references therein.
- [10] G. Belanger, F. Boudjema, A. Pukhov and A. Semenov, *Comput. Phys. Commun.* 180 (2009) 747 [arXiv:0803.2360 [hep-ph]].
- [11] Z. H. Yu, J. M. Zheng, X. J. Bi, Z. Li, D. X. Yao and H. H. Zhang, *Nucl. Phys. B* 860 (2012) 115 [arXiv:1112.6052 [hep-ph]].
- [12] A. H. Abdelhameed *et al.* [CRESST], *Phys. Rev. D* 100 (2019) 102002, no.10 [arXiv:1904.00498 [astro-ph.CO]].
- [13] M. Tanabashi *et al.* [Particle Data Group], *Phys. Rev. D* 98 (2018) 030001.
- [14] J. P. Leveille, *Nucl. Phys. B* 137 (1978) 63.
- [15] P. J. Fox, R. Harnik, J. Koppe and Y. Tsai, “LEP Shines Light on Dark Matter,” *Phys. Rev. D* 84 (2011) 014028 [arXiv:1103.0240 [hep-ph]].
- [16] R. Essig, J. Mardon, M. Papucci, T. Volansky, and Y. M. Zhong, *JHEP* 11 (2013) 167 [arXiv:1309.5084 [hep-ph]].
- [17] L. Darmeé, S. A. R. Ellis, and T. You, *JHEP* 07 (2020)

- 053 [arXiv:2001.01490 [hep-ph]].
- [18] S. Schael *et al.* [ALEPH, DELPHI, L3, OPAL and LEP Electroweak Collaborations], Phys. Rept. 532 (2013) 119 [arXiv:1302.3415 [hep-ex]].
 - [19] J. Abdallah *et al.* [DELPHI Collaboration], Eur. Phys. J. C 38 (2005) 395 [hep-ex/0406019]; J. Abdallah *et al.* [DELPHI Collaboration], Eur. Phys. J. C 60 (2009) 17 [arXiv:0901.4486 [hep-ex]].
 - [20] B. Aubert *et al.* [BaBar Collaboration], [arXiv:0808.0017 [hep-ex]].
 - [21] T. Abe *et al.* [Belle-II], [arXiv:1011.0352 [physics.ins-det]].
 - [22] M. Aaboud *et al.* [ATLAS Collaboration], JHEP 1806 (2018) 166 [arXiv:1802.03388 [hep-ex]]; A. M. Sirunyan *et al.* [CMS Collaboration], Phys. Lett. B 792 (2019) 345 [arXiv:1808.03684 [hep-ex]].
 - [23] [ATLAS Collaboration], ATLAS-CONF-2020-048.
 - [24] [CMS Collaboration], Phys. Lett. B 792 (2019) 345 [arXiv:1808.03684 [hep-ex]].
 - [25] O. Buchmueller, M. J. Dolan, S. A. Malik, and C. McCabe, JHEP 01 (2015) 037 [arXiv:1407.8257 [hep-ph]].
 - [26] C. B. Jackson, G. Servant, G. Shaughnessy, T. Tait, and M. Taoso, JCAP 07 (2013) 021 [arXiv:1302.1802 [hep-ph]].
 - [27] G. Belanger, A. Mjallal and A. Pukhov, arXiv:2003.08621 [hep-ph].
 - [28] C. Alpigiani, A. Bevan, M. Bona, M. Ciuchini, D. Derkach, E. Franco, V. Lubicz, G. Martinelli, F. Parodi, and M. Pierini *et al.*, arXiv:1710.09644 [hep-ph].
 - [29] H. Zhang *et al.* [PandaX Collaboration], Science China (Phys. Mech. Astron.) 62 (2019) 31011, no.3 [arXiv:1806.02229 [physics.ins-det]].
 - [30] D. Akerib *et al.* [LUX-ZEPLIN (LZ) Collaboration], Nucl. Instru. & Meth. A 953 (2020) 163047 [arXiv:1910.09124 [physics.ins-det]].
 - [31] E. Aprile *et al.* [XENON Collaboration], JCAP 2011 (2020) 031 [arXiv:2007.08796 [physics.ins-det]]; JCAP 1604 (2016) 027 [arXiv:1512.07501 [physics.ins-det]].
 - [32] T. P. Cheng and M. Sher, Phys. Rev. D 35 (1987) 3484
 - [33] G. Aad *et al.* [ATLAS Collaboration], Phys. Lett. B 801 (2020) 135148 [arXiv:1909.10235 [hep-ex]].